International Journal of
INTELLIGENT SYSTEMS AND APPLICATIONS IN ENGINEERING
IJISAE
ISSN:2147-6799 www.ijisae.org Original Research Paper

Design Development of Machine Learning Secure Image Transmission Based Cooperative Communication and Gaussian Elimination

Dr. Firas Husham Almukhtar

Submitted: 14/09/2022 **Accepted**: 22/12/2022

Abstract

Tumors are difficult to notice in medical imaging due to their intricate structure and noise, making it difficult and time-consuming for doctors to locate them. This is important since locating and pinpointing the tumor's site at an early stage is critical. Due to the complicated structure of tumors and the involution of noise in Magnetic Resonance Imaging (MRI) data, physical tumors identification has become a difficult and time-consuming process for medical practitioners. Thus, this paper proposes a machine learning-based approach for segmenting and categorizing of magnetic resonance images to identify brain tumors. The framework of this paper uses SVM and Naive Bayes algorithms for image pre-processing, feature extraction, and classification. The results indicated that the two classification algorithms used (Naïve Bayes and SVM) had an accuracy of 0.89 for SVM and 0.51 for naïve Bayes, a sensitivity of 0.57 and 0.85, and a specificity of 0.99 0.42, respectively. The findings indicate that SVM is more precise and specified than Naïve Bayes but that Naïve Bayes is more sensitive, with a sensitivity of 0.85. The Naïve Bayes classifier produces modest performance when compared to SVM classifiers.

Keywords: Cooperative Communication, MIMO, MRI Images, Machine Learning, Gaussian Elimination, K Means, KNN.

1. Introduction

Due to the increase of encephaloma tumors throughout all age groups. conventional knowledge says that unchecked growth in the encephalon classifies tumors as benign or malignant. Cancerous cells have multiplied in tumors labelled "malignant" because of their "non-uniform" growth pattern. According to the American Society of Clinical Pathology, regularly arranged and non-malignant cells make up benign tumors. In medical imaging, tumors are difficult to identify physically because of their complicated structure and inherent noise, making it difficult and time-consuming for specialists. Detecting and pinpointing the tumor's location at an early stage is thus very important. It is possible to follow and predict cancerous spots at various levels by employing medical scans, combined with segmentation and relegation methods to offer an early diagnosis [1], [2].

Identifying brain tumors tissues requires the time-consuming and challenging job of segmenting an MRI image. With the help of the segmentation, it is possible to identify and diagnose clinically the structures that are often muddled in medical images. The radiologist's manual examination might lead to more photographs of an inaccurate tumor's diagnosis. To eliminate the chance of human mistakes, an automated approach was necessary to analyze and relegate medical pictures [3].

A wide range of subjects is included in the study of digital image processing, including medicine, microscopy, astronomy, computer vision, and geology, to name just a few. There are several steps to the process of scientific and medical research. Medical imaging is a critical step since it enables the automated segmentation of medical images and the creation of computer-aided designs. Using human-machine interaction, they help enhance surgical treatment planning and precision. Developing imaging devices and implementing a treatment plan are two parts of this method to give useful diagnostic tools in the medical field. Segment pictures of the human anatomy were created using a variety of medical instruments. MRI and Computed Tomography (CT) are the two most often utilized noninvasive imaging modalities for capturing images of the human body [4], [5].

To develop a brain tumor, aberrant tissues must pile up over time. While these aberrant tissue types disrupt normal tissue formation, growth, and death, these abnormal tissue types cause the tissue to grow and proliferate at an uncontrolled pace. Medical Imaging (MR) modalities, including CT and MRI, are used to detect brain tumors, and CT is the most often employed. In MRI / CT scans, physicians and radiologists use three-dimensional (3D) pictures to identify a brain tumor in these images. If a computer does the analysis, for example, the computer detects the features of a brain tumors and

Department of Computer Technical Engineering, Imam Ja'afar Al-Sadiq University, Kirkuk, Iraq.
Firas.Husham@Sadiq.edu.iq

defines it in the 3D picture, which reduces the time spent by the expert and provides more consistent findings. There are several advantages to using this kind of automated/ semi-automated tumors segmentation, which helps human professionals plan patient care while concentrating on other activities [6]. Various steps involved in MRI image processing are shown below in fig. 1 using a deep learning method.

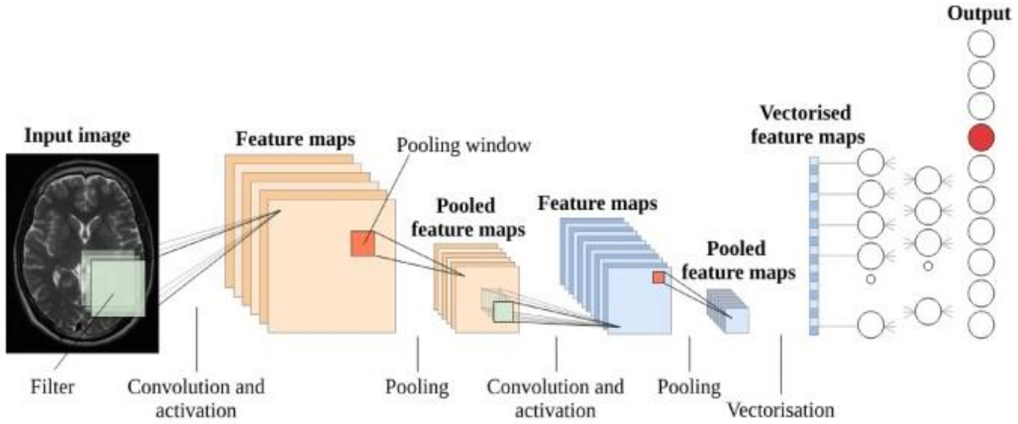

Figure 1 – Medical Images Classification using Deep Learning algorithm

Fig. 2 displays the process of deep learning dealing with images taken from the MRI, with all steps needed for the image reconstruction, restoration and registration.

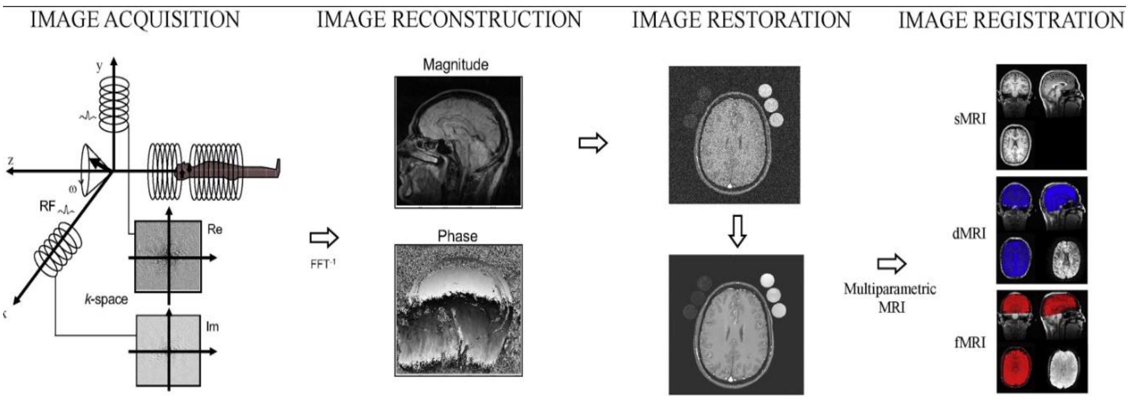

Figure 2. Deep learning in MR signal processing chain, from image acquisition (in complex-valued k-space)

Because of noise, non-brain tissues, bias fields, and other factors, complete MRI pictures are not ready for processing right away. Different pre-processing strategies are available to deal with this particular problem. Pre-processing is a time-consuming process that involves removing all of the unneeded components from the photos after they have been successfully processed [7]. Image Pre-processing includes, image conversion to grayscale [8], noise removal, and image reconstruction. Image feature extraction and classification are the steps following the preprocessing of the MRI images as shown in Fig. 3.

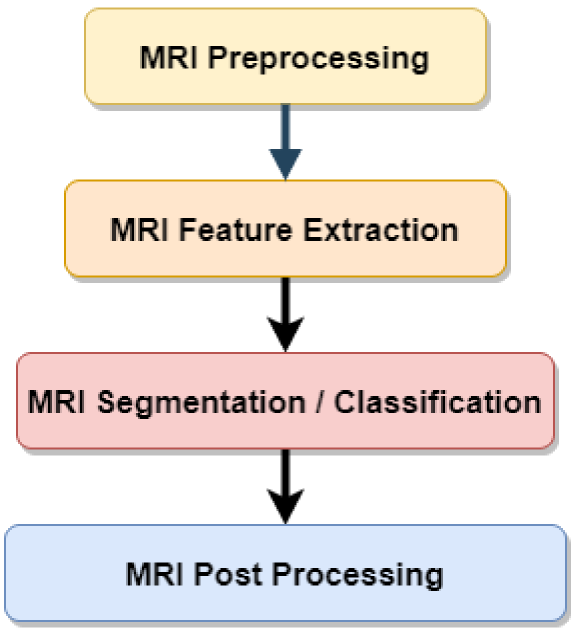

Figure 3: Steps Involved in MRI Image Processing

Several filtering methods are used to remove the surplus noise once the image has been converted to grayscale. The technique of reducing the noise becomes crucial after collecting the photographs from the database in order to produce an effective result. There are significant shortcomings in present methods for minimizing noise. [9]. other details can be constructed as:-

I. **Segmentation:** Large images were produced throughout the scanning process, and it is expected that clinical professionals will be able to identify these photos in a fair amount of time manually. Important step that plays a vital role in clinical diagnosis and is also used in pre-surgical planning and computer-assisted surgery [10].

II. **Feature Extraction:** This method entails assigning a feature vector to each image, which is subsequently likely to become its identity. Its objectives are to extract the features that optimize recognition rate with the fewest components while also establishing the same feature set for multiple instances of the same symbol, both of which are challenging to accomplish. Current feature extraction algorithms are unable to select the most significant features for further investigation [11].

III. **Classification:** It categorizes each item in a batch of data into a preset set of classes or groupings of items. A common application for this approach is to discriminate between normal and malignant brain pictures. The basic goal of classification is to accurately anticipate the target class for each case in the data. To accomplish this, it divides brain pictures into two categories: tumors and non-tumors. Because current approaches do not strongly emphasize the effective categorization of MRI images, our proposed effort will strongly emphasize this phase [1].

2. Literature Survey

There are several methods for classifying brain tumors. Among the most commonly used techniques are machine learning approaches, such as the fully convolutional network (CNN) methodology and with deep learning (DL) modes. The researchers looked at how deep characteristics collected from pre-trained CNNs may be used to predict survival time. It adds to the evidence that fine-tuning property parameters can increase performance. On the internet, there is a standard dataset as shown in Tab. 1. In the instance of start leaving cross-validation, it has an accuracy of roughly 81 percent [12].

Table 1. A short list of medical imaging data sets and repositories.

Name	Summary	Link
OpenNeuro	An open platform for sharing neuroimaging data under the public domain license. Contains brain images from 168 studies (4,718 participants) with various imaging modalities and acquisition protocols.	https://openneuro.org[a]
UK Biobank	Health data from half a million participants. Contains MRI images from 15,000 participants, aiming to reach 100,000.	http://www.ukbiobank.ac.uk/
TCIA	The cancer imaging archive hosts a large archive of medical images of cancer accessible for public download. Currently contains images from 14,355 patients across 77 collections.	http://www.cancerimagingarchive.net
ABIDE	The autism brain imaging data exchange. Contains 1114 datasets from 521 individuals with Autism Spectrum Disorder and 593 controls.	http://fcon_1000.projects.nitrc.org/indi/abide
ADNI	The Alzheimer's disease neuroimaging initiative. Contains image data from almost 2000 participants (controls, early MCI, MCI, late MCI, AD)	http://adni.loni.usc.edu/

Within the study of Mohan and Subashini [2], a hybrid strategy for identifying the components of a brain tumor image was described. In this approach, a Support Vector Machine (SVM) is employed for categorization and a Genetic Algorithm (GA) is used for feature extraction. The features are then compared to the saved features, and the technique is used to capture the photos and their visual contents. This technique employs the raw image to facilitate decision-making in a very targeted manner. Selecting the features to be merged in classification algorithms solved with the GA is a difficult task. The features are then compared to the saved features, and the technique is used to capture the photos and their visual contents.

The hybrid method was utilized to identify classifications for MRI brain tumors. In order to help doctors succeed in their therapy, this technique offers them a second point of view. There are only a few photo databases and this only works on a specific type of tumor.

The simple three approach for detecting brain cancers in MRI images was proposed inside the study. The procedure entails finding individuals with brain tumors, choosing all of their aberrant slices mechanically, then segmenting and identifying the tumor. For the first procedure, the features can be extracted using wavelet transforms (DWT) on a set of normalized pictures, which are then categorized using the SVM classifier. The second process follows the same steps as the first. Instead of using SVM, the randomized forest (RF) categorization technique is employed. Another 400 patients are split into three groups of three in a 3:1 ratio with no overlap. A single image-based configuration categorization was created by combining all of the magnetic resonance slices. It has a fresh and unique contralateral method, as well as patch thresholds for the segmentation process. This patch threshold does not necessitate the usage of training sets or templates for segmentation research. When compared to other classification approaches, the tumors are segmented with great accuracy. [6]

Deep Learning is a novel method in the machine learning sector, and it is used in a variety of challenging applications. This DL method, when paired using DWT and Principle Components Analysis (PCA), improves the categorization of brain tumors. With time, the inconvenience of not having a real-time dataset for better results grows. [9]

The work provided a deep segmentation and machine learning technique for classifying MRI brain tumor imaging images into benign and malignant tumors. When the various CNN based classification are compared to deep features and machine intelligence classification model, superior results are obtained (Kang et al., 2021). The novel approach of classifying brain tumors into normal and pathological forms is called local restriction convolution vocabulary learning. The REMBRANDT data are used for classification in this unsupervised classification approach. This strategy is far superior to the different existing methods for classifying tumors [3]

The study successfully classified images of benign and malignant brain tumors using the modified deep convolutional neural network (DCNN). This method of classification was used to accurately classify 220 patients' T1, T2, and T2 diffusion inverted recovery (FLAIR) magnetic resonance images. In the research, a method for quickly identifying MRI images of brain tumors known as DL-based opposing crow search (DL-OCS) was presented. In this technique, the classification stage's correct feature selection is viewed as being of utmost importance. The DL-OCS method performs better than the alternatives (95.22%) in terms of specificity (86.45%), specificity (100%), and accuracy. [16].

Using machine learning approaches, the researchers uncovered a number of relevant research topics in medical picture processing. Machine learning systems aid in the preservation of health records in electronic files, which is growing with time. The benefits of digitizing medical photos include accuracy, up-to-date information, rapid access, increased reliability, ease of sharing, improved safety and confidentiality, lower expenses, and so on. The paucity of datasets for computer - aided diagnostic training is a major challenge. Furthermore, due to the data imbalance or inadequate training sets, it is difficult to detect uncommon illnesses with high accuracy [19].

2.1 Pre-processing Techniques

Image processing can be used to examine brain images. Magnetic Resonance Imaging (MRI) is a tool that doctors utilize for a variety of diagnostic and therapeutic operations. The following steps are involved in pre-processing of an image: Improving noise reduction and removing artefacts. This image should make it simple to locate tumors. For astrocytoma-related MRI brain images, the Suryavamsi et al. [12] team proposed three methods: "Histogram Equalization," "Adaptive Histogram Equalization," and "Brightness-Preserving Dynamic Fuzzy Histogram Equalization." Performance measures have been used to calculate the outcomes of these three approaches (RMSE, MSE, and PSNR).

Background noise must be eliminated from MRI data before the required signal can be retrieved. Several pre-processing processes rely on nuisance regression and independent component analysis. De Blasi et al. [13] eliminate non-BOLD signals from healthy people and patients with temporal lobe epilepsy using a variety of LD cleaning processes. All pre-processing processes evaluated enhanced temporal characteristics, such as SNR and power spectrum density in the resting-state frequency range, relative to pre-processed data (0.01-0.1 Hz). As part of the pre-ICA procedure, the pre-processing pipeline was inspected to locate the DMN. Compared to other pipelines and groups, these pipelines and groups were able to characterize better the posterior region of the cingulate cortex [10], [11], [14], [15].

Poornachandra and Naveena [16] enhanced pre-processing methods to segregate glioma tumors efficiently. Tumors in the brain Medical Imaging have recently been produced using cutting-edge Deep Learning techniques. Thanks to superior segmentation results, researchers with a greater understanding of brain tumors are better able to detect the ailment and give treatment options to patients who have been diagnosed with it.

The use of brain MR imaging to detect and segment the tumor's anatomy has sparked much debate. Image segmentation is difficult because of the image's consistency. Widyarto et al. [15] enhanced the Region Scalable Fitting technique for image segmentation by incorporating pre-processing before using a region-based active contour model. Models based on intensity data are employed in some regions. Preprocessing ensures that the two-dimensional-sigmoid function is maintained at the tumor boundary. In the pre-processing steps of the brain MRI picture, an extra 2D-sigmoid function increased the contrasts.

2.2 Feature extraction techniques

One of the most critical steps in tumor segmentation systems is extracting important properties.

To improve brain tumor segmentation accuracy, Jui et al. [11] developed an upgraded feature extraction component that considers the link between intracranial structural deformation and compression as a consequence of brain tumor expansion. Non-rigid registration and deformation modelling are used to distort 3D volumetric pictures in the LaV region of the brain. LaV deformation feature data on brain tumor segmentation may be confirmed and enforced using frequently utilized classification methods, such as k-means in a quantitative and qualitative examination of the proposed component; the author found positive results [5].

J. Zhang [17] apply the strategy of feature extraction as a diagnosis utility work on longitudinal structural MR images which does not involve nonlinear registration or tissue segmentation. To quickly and accurately identify landmarks in test images, we use a nonlinear registration and tissue segmentation-free technique. We can now describe the brain's structural absorption in spatial terms by integrating high-level statistical traits and longitudinal contextual factors. The Alzheimer's Disease Neuroimaging Initiative database showed a classification accuracy of 88.30 percent for Alzheimer's disease and Mild Cognitive Impairment (MCI) when we used our proposed approach, superior performance, and efficiency.

A comprehensive, automated breast CAD system developed by Piantadosi et al. [18] to aid in the detection of breast cancer. In a design given by Piantadosi et al. [18], the modules for breast segmentation, motion artefact attenuation, lesions localization, and classification based on their malignancy are included. In order to provide a fair comparison, 42 individuals with proven histological lesions were chosen for cross-validation. According to the findings of the studies, there is no need for human intervention in any of the processing stages of the BLADeS system's breast lesion diagnosis.[19].

Tsai et al. proposed a parallelization of feature extraction using the Gray-Level Co-Occurrence Matrix (GLCM) [20]. Instead of being built and optimized on a single computer, this solution uses several GPUs to run the code. When testing on Geforce GTX 1080s with single-precision MR brain pictures and double-precision MR brain images, the proposed approach is more than 25-105 times quicker than its serial equivalent, depending on the size of the ROIs [10].

2.3 Segmentation techniques

A Convolution Neural Networks (CNN)-based automated segmentation method that looks at the tiny 3 x 3 kernels was proposed by Pereira et al. [21]. The network's smaller number of weights not only helps minimize overfitting, but also makes it possible to design a more intricate architecture. Even though this pre-processing step is unusual in CNN-based segmentation methods, it has been found to be quite successful when used with data augmentation for the segmentation of brain tumors in MRI images.

Kim et al. [22] introduced a semi-automatic segmentation technique that uses the better picture quality provided by ultrahigh field (7T) MRI. This strategy used the complementary edge information from different structural MRI modalities. SUS, T2 and diffusion MRI are linked, and a novel edge indicator function is developed using the data from all three modalities. The design and architecture of the subcortical structures aid in the evolution of active geometric surfaces. A non-overlapping penalty was imposed on over-segmentation at the borders of neighboring structures [22].

Early preterm to term-equivalent age should be classified into 50 separate brain areas, according to Markopoulos et al. [8]. Here, the structural hierarchy and anatomical constraints are considered using a unique segmentation approach to simulate intensity over the entire brain. This approach differs from traditional atlas-based strategies in that it improves label overlaps in terms of manual reference segmentations. Experiment findings show that the suggested method is reliable throughout many gestational ages, from 24 weeks to term-equivalent.

3. Proposed Framework

Fig. 4 depicts the suggested framework. Filtering and enhancing the image is required to improve it. When utilizing images taken with a cell phone, a range of circumstances may impact the segmentation results. Preprocessing includes picture scaling, noise removal, and image enhancement. A digital picture may contain many sounds. This may cause picture noise, rendering simple thresholding useless. Image noise must be decreased. Image noise refers to random variations in a picture's lighting or hues. Images may contain Gaussian, salt and pepper, shot and quantized noise, and other types of noise. These glitches may be removed by using filters such as the median and Wiener. Noise reduction may be accomplished using a number of morphological approaches. The brightness of individual pixels is affected differently by median and Gaussian Filtering (GF). In this case, Gaussian Filtering was used to minimize noise. Gaussian filtering replaces the importance of each pixel's intensity with a weighted average of the brightness of neighboring pixels. [10].

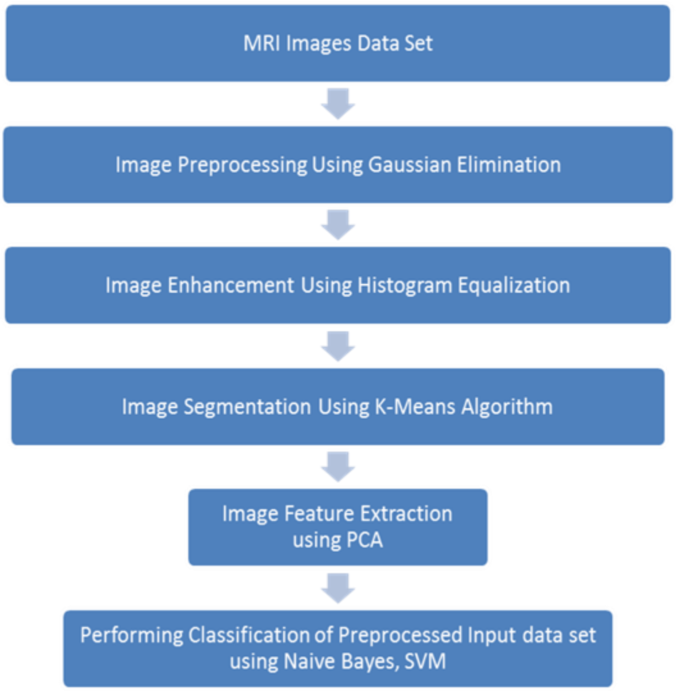

Figure 4: A Framework for MRI Image Segmentation and Classification

Images improve information reflection or human interpretability after filtering to enable better image processing. Equalizing the histogram of the input image results in a uniform intensity distribution and a consistent histogram. Using this strategy consistently enhances the universal contrast of photographs, especially when the experimental data for the image is close to contrast. This method may distribute the intensity of the histogram uniformly. As a result, low-contrast regions gain local contrast. The picture is completed by dispersing the most frequent intensities by equalizing histograms [14].

In order to obtain the correct Region of Interest (ROI), the picture is first improved using dynamic fuzzy histogram equalization and then segmented. Important characteristics may be found by analyzing these portions. In picture segmentation, comparable parts of an image are identified and grouped. There are both region-based and edge-based segmentation methods. By evaluating intensity patterns surrounded by a cluster of surrounding pixels, it is feasible to detect anatomical or functional elements. [23].

Using region-based segmentation, the ROI is split into portions according to its texture or pattern. The local mean is used as a cluster pattern in k-means clustering for a set of k different interpretations of a given data set. To identify groups in data, the sum of the groups represented by the variable k is utilized. Euclidean distances are used to find the nearest data. Data points are allocated to one of the k groups based on the characteristics supplied. [24], [25], [26].

Vapnik's invention of SVM has drawn the interest of scientists all around the world. Data is gathered and divided into two groups by an SVM classifier. A model is constructed for testing once the classifier has been trained on some training data. Categorization into more than one class is not unheard of. Binary classifiers are going to be in high demand. SVM has been found to outperform other current classification algorithms in several studies. Using SVM, you can categorize photographs. In terms of accuracy, SVMs surpass a variety of other classifiers [26].

4. METHODOLOGY

In the suggested system. Principal Component Analysis (PCA) is used to transform feature extraction while K-means clustering is used to segment MRI brain pictures. The K-nearest neighbor approach is used to categorize normal and pathological tissue, and the whole process is depicted in Fig. 5. The clustering strategy is used in the categorization of MRI images. The goal of the k-means method is to arrange objects into n clusters depending on their attributes. To calculate the cluster, the centroid of the cluster and the sum of the squares of the distances between the data are taken into account. In this method, the k number of clusters must be defined initially, and the randomized clusters created from the n elements must subsequently be fixed. It is utilized here to use the Euclidean function.

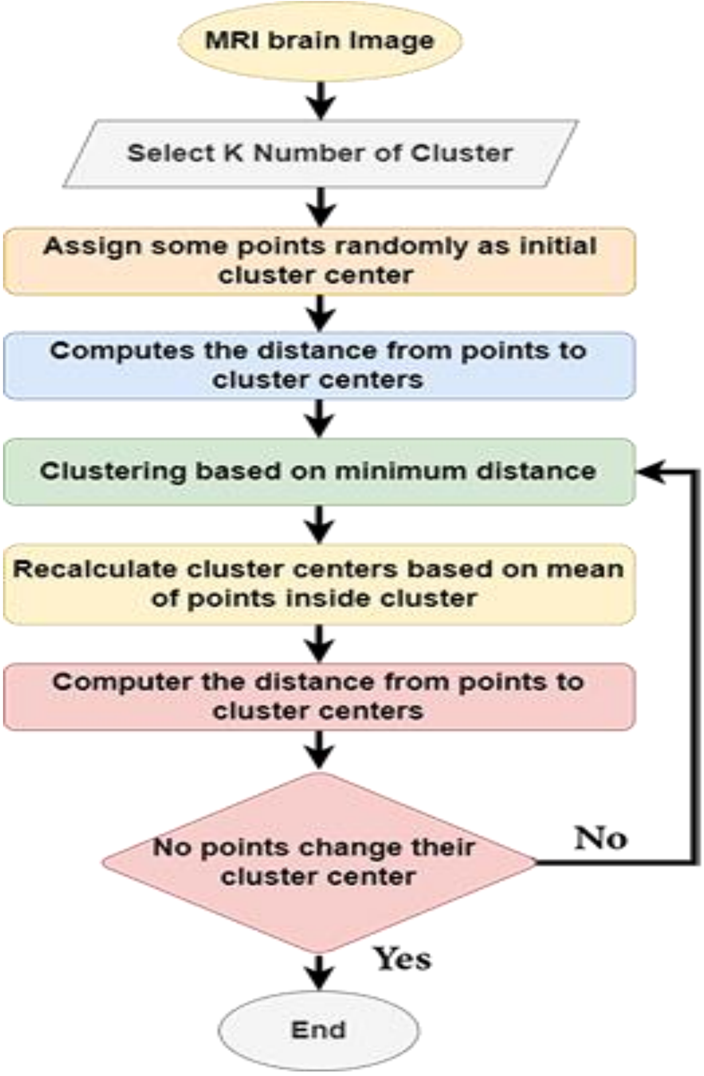

Figure 5 - Flow Chart Of K-Means Algorithm

Using the algorithm below, one pixel is compared to the centers of all clusters to get the distance between each pixel and each cluster. [19]

$$M= K=1\ldots\ldots K \qquad (1)$$

$$D(I) = \text{Avg Min}||Xi\text{-}Mk||^2, \quad I=1\ldots\ldots N \qquad (2)$$

After that, the pixel is shifted to the group with the minimum distance between all of them, and the centroid is recalculated. Each image is matched to all centroids once more, and the procedure is repeated until the centroid converges.

Principal Component Analysis (PCA) - In real coordinate space, a collection of points is represented by a sequence of p unit vectors, with the i-th vector denoting the direction of a line that best fits the data while being orthogonal to the first i-1 vectors. The average squared distance between the points and the line, in this situation, is what determines which line is the best match. These directions create an orthonormal foundation for the data, in which the different dimensions are not linearly connected. In principle component analysis (PCA), the principal components are calculated and used to alter the data's underlying structure. Frequently, the first few principal components are used, with the other principal components being ignored.

Following the PCA algorithm, another two methods are utilized to perform the classification process, these are SVM and Naïve bias which can be described as follows: -

Support Vector Machine (SVM): - enables the use of supervised machine learning to tackle classification and regression issues. But classification problems are what it's used for most of the time. Each piece of data is represented as a point in an n-dimensional space (n is the number of features you have), with each feature's value being the value of a particular position in the SVM method. Locating the hyper-plane that clearly separates the two groups allows us to complete classification.

Naïve Bias Classifier (NB): - A probabilistic machine learning model is utilized to perform classification tasks. The Bayes theorem is the cornerstone of the classifier..

$$\boldsymbol{P(A|B) = \frac{P(B|A)P(A)}{P(B)}} \qquad \ldots\ldots(\mathbf{3})$$

Using Bayes' theorem, we may determine the likelihood of A occurring if B has previously occurred. The hypothesis is A, and the proof is B. In this situation, the predictors/features are supposed to be independent. That is, the existence of one quality has no effect on the presence of another. As a result, it is said to as naive.

5. Result Analysis

K-means grouping with the aid of SVM and Naiv Bays algorithms are used to judge the effectiveness of brain tumor classification. The collection of MRI images that was utilized in the visual segmentation algorithm. There are 40 tumors involved in the MRI scans used in this article. Initially, two clusters were allocated in the k-means technique, however it was discovered that tumor pixels were not segregated properly, therefore three clusters were added afterwards. The tumor component was clearly segregated from the healthy cells in the final photos. Figures 6 and 7 show, respectively, brain MRIs for cancer and benign conditions.

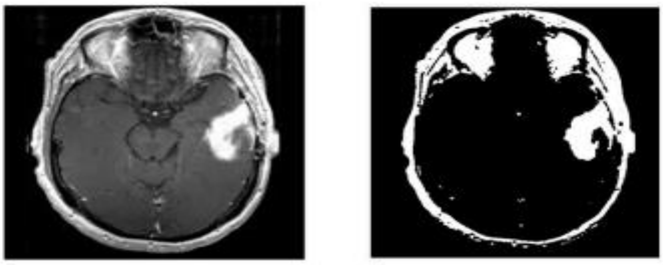

(a) (b)

Figure 6 – Images of a malignant brain MRI (a) and a tumor (b)

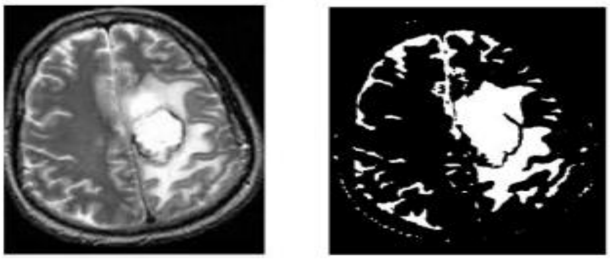

(a) (b)

Figure 7 – (A) Original Image (B) Tumor Image: Benign Brain MRI

"Dataset-160 and Data-255" from Harvard's clinical college of "architecture" have been analyzed. As part of our analysis, we looked at datasets 160, 255, and 35, including "Normal-20" and "Abnormal-140" MR256x256 axial aero plane encephalon pictures. The "Dataset-255" Irregular Encephalon Magnetic Resonance metaphors represent eleven distinct symptoms and link to the "Dataset-160" by linking the seven distinct syndromes. "Dataset-160" includes cases of agnosia, glioma, meningioma, Pick's infection, and sarcoma in addition to Huntington's syndrome, Alzheimer's infection, and Alzheimer's sickness. Herpes encephalitis, chronic subdural hematoma, and various forms of sclerosis are among the four novel conditions documented in "Dataset-255". "Dataset-255". The following are the formulas that were used to performance parameter:

1. ***Sensitivity***:

$$\text{Sensitivity} = \frac{\text{TP}}{(\text{TP}+\text{FN})} \qquad \text{.....} \qquad (4)$$

Where TP stands for True Positive that represents Pixels from Tumors (type I error) and FN stands for False Negative which represent incorrect non-tumor pixels (type II error).

2. ***Specificity:***

$$\text{Specificity} = \frac{\text{TN}}{(\text{TN}+\text{FP})} \qquad \text{......} \qquad (5)$$

Where TN stands for True Negative and FP stands for False Positive

3. ***Accuracy***

$$\text{Accuracy} = \frac{\text{TN}+\text{TP}}{(\text{TN}+\text{TP}+\text{FN}+\text{FP})} \qquad \text{.......(6)}$$

The tumor images and non-tumor images were separated by the pixels in the classification method. True positive photons are tumor pixels, whereas Real negative pixels are quasi pixels. During the segmentation stage, a limited handful of tumor pixels and non-tumor pixels was jumbled together, resulting in false negatives pixels. The accuracy factor is computed for both procedures, and 85 percent accuracy is reached.

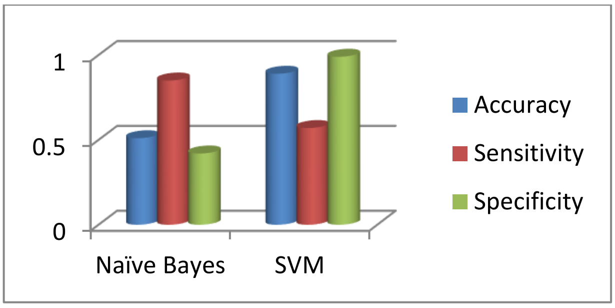

Figure 8: Result Comparison of Classifiers

The performance of several classifiers is illustrated in Figure 9, Figure 10, and Table 2. Three metrics are compared: accuracy, specificity, and sensitivity.

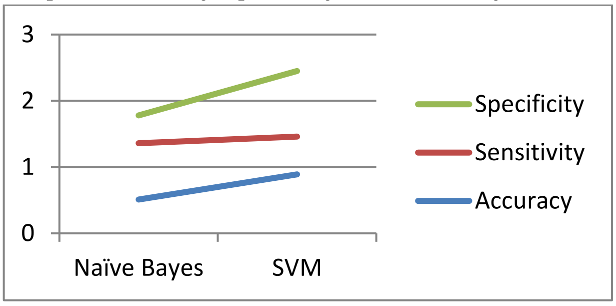

Figure 9: Accuracy, Sensitivity and Specificity for Medical Image Classification

Table 2: Comparison of SVM and Naïve Bayes for Medical Image Classification

Algorithm Name	Accuracy	Sensitivity	Specificity
SVM	**0.89**	**0.57**	**0.99**
Naïve Bayes	**0.51**	**0.85**	**0.42**

The following figure may be used to compare the SVM and Naive Bais throughout the training level

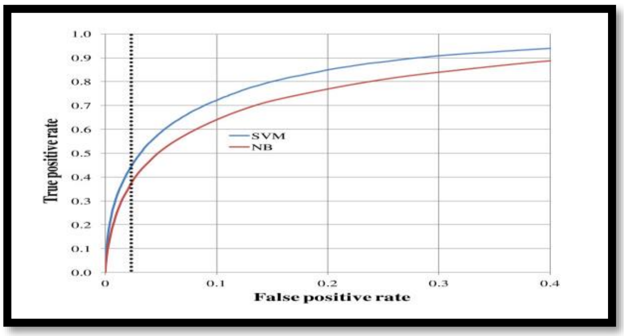

Figure 10: Comparison of SVM and Naive Base at training level

6. Discussion

This study aimed to design and develop a machine learning and image segmentation-based model to classify medical images efficiently. Figures 8,9,10 and Table 2 compared the two classification algorithms (Naïve Bayes and SVM) with an accuracy of 0.89 for SVM and 0.51 for naïve Bayes, 0.57 and 0.85 sensitivity 0.99 0.42 specificity, respectively. The findings show SVM is more accurate and specified than Naïve Bayes, while Naïve Bayes is more sensitive with 0.85. Using Naïve Bayes and SVM on the dataset, the results are shown in Table 2. The Multinomial variation was used to test the Naïve Bayes classifier for the first time. According to the data, the classifier was able to come accurately at around 0.89 and 0.51, similar to the finding of Liu et al. [27]. The findings are contrary to Hlaing et al. [28], who indicated that Naïve Bayes forms of Naïve Bayes can produce good results in Sentiment Analysis. To be fair, when compared to the SVM classifiers, the Naive Bayes classifier yields moderate results. As previously noted, we assess the Support Vector Machine and Naïve Bayes using the accuracy, sensitivity and specificity [16].

This site's accuracy can be gauged by looking at the percentage of correctly classified medical photos. These two methods can be used to demonstrate the effectiveness of the binary classification algorithm. The support vector machine (SVM) was widely accepted as a universal classifier. Two types of SVM concatenations will be compared to the Conditional Neural Movement Primitives (CNMP) model: the traditional SVM and the deep SVM. The table demonstrates that Nave Bayes is more accurate than SVM (the standard feature) [29]. A medical look can be accurately depicted by high-level traits, as evidenced by findings like these. Because images can be perceived from a multiscale perspective by combining features from both methods, combining the features from both methods can be an effective strategy [30].

Xu et al. [31] show that increasing the number of picture samples impacts the performance of the deep model. However, the authors did not conduct more qualitative studies into this issue. Increasing the number of photos will cause all algorithms to take longer, as predicted by Menze et al. [3].

According to Zhifei et al. [15], computer-aided segmentation of vital organs, tissues, or lesions from medical images is necessary to assist physicians in making accurate diagnoses. Numerous medical imaging datasets and competitions have been generated to foster the development of computer-aided diagnosis systems. The development of deep learning techniques has simplified developing multi-organ analysis models. Unlike conventional organ-specific segmentation techniques, multi-organ segmentation models incorporate interactions across many organs to more accurately depict the complex human anatomy. Additionally, numerous metrics for evaluating the segmentation effectiveness of medical image segmentation models have been devised. Image segmentation performance is quantified in pixel, region, and surface distance quality [32].

Medical imaging is frequently accompanied by significant background noise. It is significantly more expensive to annotate medical images than with nature photographs. Thus, the segmentation of medical images using deep learning models trained on natural images is an exciting research field [33]. Transfer learning is especially advantageous for segmenting medical images with less supervision. Indeed, transfer learning is predicated on discovering parallels between previously acquired and newly acquired knowledge. Transfer learning enables us to share model parameters (or knowledge learnt by the model) with the new model because most data and tasks are connected. Thus, transfer learning can help address the issue of unlabeled data [4].

Numerous studies demonstrate that deep learning is commonly employed in medical image segmentation. Breast tissue segmentation was performed solely through the use of deep learning. While incorporating deep learning algorithms into medical imaging is exciting, progress is slow. In medical image analysis, deep learning is restricted by precise annotations of medical pictures [16].

7. Conclusion

A rise in encephaloma tumors in each age group has increased the fatality rate. The complex nature of tumors and noise in MR imaging data make physical tumor detection challenging and time-consuming for doctors. As a result, early detection and localization of the tumor are critical. Medical scans can be used with segmentation and relegation techniques to detect cancer tumors at various levels. Our system uses machine learning to classify MRI images for brain tumor identification. This framework comprises SVM and Nave Bayes algorithms for image pre-processing, segmentation, feature extraction, and classification. Further research is required to improve the algorithm's accuracy, sensitivity, and specificity using more images.

A percentage of 87% accuracy has been achieved successfully by implementing k-mean clustering to segment the images acquired for the MRI of the brain. It is recognized, nonetheless, that the features chosen affect how accurate a machine learning system is. Other MRI image, such as those for liver cancer, lung cancer, breast cancer, and bladder cancer, can be detected using our suggested methodology. Future work on this topic will involve testing and training the algorithm on numerous datasets and comparing the results to those of other methods. In the future, neural networks may also be used for the diagnosis of brain tumors.

Declarations:

Availability of data and material: Not applicable.

Competing interests: The author declare that they have no competing interests

Funding Statement: The author received no specific funding for this study.

Authors' contributions: Corresponding author contributed significantly to the research and this paper.

Acknowledgements: Not applicable

References

[1]. S. Bauer, R. Wiest, L. P. Nolte, and M. Reyes, “A survey of MRI-based medical image analysis for brain tumor studies,” *Phys. Med. Biol.*, vol. 58, no. 13, Jul. 2013, doi: 10.1088/0031-9155/58/13/R97.

[2]. G. Mohan and M. M. Subashini, “MRI based medical image analysis: Survey on brain tumor grade classification,” *Biomed. Signal Process. Control*, vol. 39, pp. 139–161, Jan. 2018, doi: 10.1016/J.BSPC.2017.07.007.

[3]. B. H. Menze *et al.*, “The Multimodal Brain Tumor Image Segmentation Benchmark (BRATS),” *IEEE Trans. Med. Imaging*, vol. 34, no. 10, pp. 1993–2024, Oct. 2015, doi: 10.1109/TMI.2014.2377694.

[4]. J. Cheng *et al.*, “Enhanced Performance of Brain Tumor Classification via Tumor Region Augmentation and Partition,” *PLoS One*, vol. 10, no. 10, p. e0140381, Oct. 2015, doi: 10.1371/JOURNAL.PONE.0140381.

[5]. G. Litjens *et al.*, “A survey on deep learning in medical image analysis,” *Med. Image Anal.*, vol. 42, pp. 60–88, Dec. 2017, doi: 10.1016/J.MEDIA.2017.07.005.

[6]. J. Sachdeva, V. Kumar, I. Gupta, N. Khandelwal, and C. K. Ahuja, “A package-SFERCB- ‘Segmentation, feature extraction, reduction and classification analysis by both SVM and ANN for brain tumors,’” *Appl. Soft Comput.*, vol. 47, pp. 151–167, Oct. 2016, doi: 10.1016/J.ASOC.2016.05.020.

[7]. S.-L. Jui *et al.*, ‘Brain MRI Tumor Segmentation with 3D Intracranial Structure Deformation Features’, *Intelligent Systems, IEEE*, vol. 31, pp. 66–76, Mar. 2016.

[8]. A. Makropoulos *et al.*, “Automatic whole brain MRI segmentation of the developing neonatal brain,” *IEEE Trans. Med. Imaging*, vol. 33, no. 9, pp. 1818–1831, 2014, doi: 10.1109/TMI.2014.2322280.

[9]. M. Ravikumar, B. J. Shivaprasad, and D. S. Guru, “Enhancement of MRI Brain Images Using Fuzzy Logic Approach,” *Commun. Comput. Inf. Sci.*, vol. 1381 CCIS, pp. 131–137, 2021, doi: 10.1007/978-981-16-0493-5_12.

[10]. Z. Iqbal, M. A. Khan, M. Sharif, J. H. Shah, M. H. ur Rehman, and K. Javed, “An automated detection and classification of citrus plant diseases using image processing techniques: A review,” *Comput. Electron. Agric.*, vol. 153, pp. 12–32, Oct. 2018, doi: 10.1016/J.COMPAG.2018.07.032.

[11]. E. S. Biratu, F. Schwenker, Y. M. Ayano, and T. G. Debelee, “A Survey of Brain Tumor Segmentation and Classification Algorithms,” *J. imaging*, vol. 7, no. 9, Sep. 2021, doi: 10.3390/JIMAGING7090179.

[12]. R. V. Suryavamsi, L. S. T. Reddy, S. Saladi, and Y. Karuna, “Comparative Analysis of Various Enhancement Methods for Astrocytoma MRI Images,” *Proc. 2018 IEEE Int. Conf. Commun. Signal Process. ICCSP 2018*, pp. 812–816, Nov. 2018, doi: 10.1109/ICCSP.2018.8524441.

[13]. B. De Blasi *et al.*, “Pipeline comparison for the pre-processing of resting-state data in epilepsy,” *Eur. Signal Process. Conf.*, vol. 2018-September, pp. 1137–1141, Nov. 2018, doi: 10.23919/EUSIPCO.2018.8553119.

[14]. W. Zhao and J. Wang, “A new method of the forest dynamic inspection color image sharpening process,” *ICACTE 2010 - 2010 3rd Int. Conf. Adv. Comput. Theory Eng. Proc.*, vol. 4, 2010, doi: 10.1109/ICACTE.2010.5579715.

[15]. S. Widyarto, S. R. B. Kassim, and W. K. Sari, “2D-sigmoid enhancement prior to segment MRI glioma tumour: Pre-image-processing,” *Int. Conf. Electr. Eng. Comput. Sci. Informatics*, vol. 2017-December, Dec. 2017, doi: 10.1109/EECSI.2017.8239103.

[16]. S. Poornachandra and C. Naveena, “Pre-processing of MR Images for Efficient Quantitative Image Analysis

Using Deep Learning Techniques," *Proc. - 2017 Int. Conf. Recent Adv. Electron. Commun. Technol. ICRAECT 2017*, pp. 191–195, Oct. 2017, doi: 10.1109/ICRAECT.2017.43.

[17]. J. Zhang, M. Liu, L. An, Y. Gao, and D. Shen, "Alzheimer's disease diagnosis using landmark-based features from longitudinal structural MR images," *IEEE J. Biomed. Heal. Informatics*, vol. 21, no. 6, pp. 1607–1616, Nov. 2017, doi: 10.1109/JBHI.2017.2704614.

[18]. F. H. Almukhtar, "Principal Component Analysis and K-Nearest Neighbor Classifier for Facial Expression Recognition System," *Int. J. Curr. Res. Acad. Rev.*, vol. 6, no. 5, pp. 17–20, May 2018, doi: 10.20546/IJCRAR.2018.605.004.

[19]. M. Osadebey, M. Pedersen, D. Arnold, and K. Wendel-Mitoraj, 'No-Reference Quality Measure in Brain MRI Images using Binary Operations, Texture and Set Analysis', *IET Image Processing*, vol. 11, pp. 672–684, Sep. 2017, doi: 10.1049/iet-ipr.2016.0560.

[20]. H.-Y. Tsai, H. Zhang, C.-L. Hung, and G. Min, 'GPU-Accelerated Features Extraction From Magnetic Resonance Images', *IEEE Access*, vol. 5, pp. 22634–22646, 2017, doi: 10.1109/ACCESS.2017.2756624.

[21]. S. Pereira, A. Pinto, V. Alves, and C. A. Silva, "Brain Tumor Segmentation Using Convolutional Neural Networks in MRI Images," *IEEE Trans. Med. Imaging*, vol. 35, no. 5, pp. 1240–1251, May 2016, doi: 10.1109/TMI.2016.2538465.

[22]. J. Kim, C. Lenglet, Y. Duchin, G. Sapiro, and N. Harel, "SEMI-AUTOMATIC SEGMENTATION OF BRAIN SUBCORTICAL STRUCTURES FROM HIGH-FIELD MRI," *IEEE J. Biomed. Heal. informatics*, vol. 18, no. 5, p. 1678, Sep. 2014, doi: 10.1109/JBHI.2013.2292858.

[23]. M. Mittal, M. Arora, T. Pandey, and L. M. Goyal, "Image Segmentation Using Deep Learning Techniques in Medical Images," pp. 41–63, 2020, doi: 10.1007/978-981-15-1100-4_3.

[24]. B. N. Mohammed, F. H. Al-Mukhtar, R. Z. Yousif, and Y. S. Almashhadani, "Automatic Classification of Covid-19 Chest X-Ray Images Using Local Binary Pattern and Binary Particle Swarm Optimization for Feature Selection," *Cihan Univ. Sci. J.*, vol. 5, no. 2, pp. 46–51, Nov. 2021, doi: 10.24086/CUESJ.V5N2Y2021.PP46-51.

[25]. Z. Deng, X. Zhu, D. Cheng, M. Zong, and S. Zhang, "Efficient kNN classification algorithm for big data," *Neurocomputing*, vol. 195, pp. 143–148, Jun. 2016, doi: 10.1016/J.NEUCOM.2015.08.112.

[26]. E. Suryawati *et al.*, "Unsupervised feature learning-based encoder and adversarial networks," *J. Big Data*, vol. 8, no. 1, pp. 1–17, Dec. 2021, doi: 10.1186/S40537-021-00508-9/TABLES/4.

[27]. M. Galety, F. H. Al Mukthar, R. J. Maaroof, and F. Rofoo, "Deep Neural Network Concepts for Classification using Convolutional Neural Network: A Systematic Review and Evaluation," *Tech. Rom. J. Appl. Sci. Technol.*, vol. 3, no. 8, pp. 58–70, Sep. 2021, doi: 10.47577/TECHNIUM.V3I8.4554.

[28]. Z. H. Moe, T. San, M. M. Khin, and H. M. Tin, "Comparison of Naive Bayes and Support Vector Machine Classifiers on Document Classification," *2018 IEEE 7th Glob. Conf. Consum. Electron. GCCE 2018*, pp. 285–286, Dec. 2018, doi: 10.1109/GCCE.2018.8574785.

[29]. S. H. Ismael, S. W. Kareem, and F. H. Almukhtar, "Medical Image Classification Using Different Machine Learning Algorithms," *Mosul Univ.*, vol. 14, no. 1, pp. 135–147, May 2020, doi: 10.33899/CSMJ.2020.164682.

[30]. Z. Lai and H. Deng, "Medical Image Classification Based on Deep Features Extracted by Deep Model and Statistic Feature Fusion with Multilayer Perceptron ," *Comput. Intell. Neurosci.*, vol. 2018, 2018, doi: 10.1155/2018/2061516.

[31]. N. Xu, W. Shan, J. Qi, J. Wu, and Q. Wang, "Presurgical Evaluation of Epilepsy Using Resting-State MEG Functional Connectivity," *Front. Hum. Neurosci.*, vol. 15, p. 364, Jul. 2021, doi: 10.3389/FNHUM.2021.649074/BIBTEX.

[32]. D. Y. Mikhail, F. H. Al-Mukhtar, and S. W. Kareem, "A Comparative Evaluation of Cancer Classification via TP53 Gene Mutations Using Machin Learning," *Asian Pacific J. Cancer Prev.*, vol. 23, no. 7, pp. 2459–2467, Jul. 2022, doi: 10.31557/APJCP.2022.23.7.2459.

[33]. M. Z. AL-Dabagh and D. F. H. AL-Mukhtar, "Breast Cancer Diagnostic System Based on MR images Using KPCA-Wavelet Transform and Support Vector Machine," *Int. J. Adv. Eng. Res. Sci*., vol. 4, no. 3, pp. 258–263, 2017, doi: 10.22161/IJAERS.4.3.41.